Search for $\eta_c(2S) \to p\bar{p}$ and branching fraction measurements of $\chi_{cJ} \to p\bar{p}$ via $\psi(2S)$ radiative decays

M. Ablikim *et al.*[*]
(BESIII Collaboration)

(Received 24 October 2024; accepted 22 November 2024; published 8 January 2025)

Using $(27.12 \pm 0.14) \times 10^8$ $\psi(2S)$ events collected by the BESIII detector operating at BEPCII, we search for the decay $\eta_c(2S) \to p\bar{p}$ via the process $\psi(2S) \to \gamma\eta_c(2S)$ and only find a signal with a significance of 1.7σ. The upper limit of the product branching fraction at the 90% confidence level is determined to be $\mathcal{B}(\psi(2S) \to \gamma\eta_c(2S)) \times \mathcal{B}(\eta_c(2S) \to p\bar{p}) < 2.4 \times 10^{-7}$. The branching fractions of $\chi_{cJ} \to p\bar{p}$ $(J = 0, 1, 2)$ are also measured to be $\mathcal{B}(\chi_{c0} \to p\bar{p}) = (2.51 \pm 0.02 \pm 0.08) \times 10^{-4}$, $\mathcal{B}(\chi_{c1} \to p\bar{p}) = (8.16 \pm 0.09 \pm 0.25) \times 10^{-4}$, and $\mathcal{B}(\chi_{c2} \to p\bar{p}) = (8.33 \pm 0.09 \pm 0.22) \times 10^{-4}$, where the first uncertainty is statistical and the second systematic.

DOI: 10.1103/PhysRevD.111.012003

I. INTRODUCTION

Experimental and theoretical studies of charmonium states play an important role in understanding quantum chromodynamics (QCD). Since the first member of this family, the J/ψ, was observed in experiment [1–3], other charmonium states below the open-charm threshold have been discovered. Among these states, the $\eta_c(2S)$ and $h_c(1P)$ are less well understood. The spin-singlet state $\eta_c(2S)$ was first observed by the Belle experiment in B meson decay $B \to K\eta_c(2S)$, via $\eta_c(2S) \to K^0_S K^{\pm}\pi^{\mp}$ [4]. This state was subsequently confirmed in several experiments [5–8]. In 2012, BESIII observed $\eta_c(2S)$ in the radiative transition $\psi(2S) \to \gamma\eta_c(2S)$, where $\eta_c(2S)$ is reconstructed by $K^0_S K^{\pm}\pi^{\mp}$ and $K^+K^-\pi^0$ final states [9]. Our understanding of $\eta_c(2S)$ decay modes is still limited. To date, only seven decay modes of $\eta_c(2S)$ have been observed experimentally, with the largest branching fraction of $(1.9 \pm 1.2)\%$ for the $K\bar{K}\pi$ mode [10].

Among the various decay channels, the decay of $\eta_c(2S)$ into a proton-antiproton $(p\bar{p})$ pair has attracted particular interest. In 2013, the decay $\eta_c(2S) \to p\bar{p}$ was searched for using 106×10^6 $\psi(2S)$ events collected by the BESIII detector [11]. The statistical significance of the $\eta_c(2S)$ signal was found to be 1.7σ, and the upper limit of the product branching fraction $\mathcal{B}(\psi(2S) \to \gamma\eta_c(2S)) \times \mathcal{B}(\eta_c(2S) \to p\bar{p})$ at the 90% confidence level (CL) determined to be 1.4×10^{-6}. The first observation of $\eta_c(2S) \to p\bar{p}$ was reported by the LHCb experiment with a statistical significance of 6.4σ, where the $\eta_c(2S)$ resonance is produced in the decay $B^+ \to [c\bar{c}]K^+$. The product branching fraction normalized to the J/ψ intermediate state is given as $\frac{\mathcal{B}(\psi(2S)\to\eta_c(2S)K^+)\times\mathcal{B}(\eta_c(2S)\to p\bar{p})}{\mathcal{B}(\psi(2S)\to J/\psi K^+)\times\mathcal{B}(J/\psi\to p\bar{p})} = (1.58 \pm 0.33 \pm 0.09) \times 10^{-2}$ [12].

Theoretically, Brodsky and Lepage [13] predict that total hadron helicity is conserved in large momentum transfer processes, implying the decays of $\eta_c(1S)/\chi_{c0}/h_c/\eta_c(2S)$ to $p\bar{p}$ are forbidden by the helicity selection rule in massless QCD models. Another topic of interest in charmonium decays is the branching fraction ratio. As spin-singlet partners of $\psi(2S)$ and J/ψ, the $\eta_c(2S)$ and $\eta_c(1S)$ can decay into light hadrons similarly. Anselmino *et al.* [14] assumed for all unforbidden hadronic channels that $\frac{\mathcal{B}(\eta_c(2S)\to h)}{\mathcal{B}(\eta_c(1S)\to h)} \approx \frac{\mathcal{B}(\psi(2S)\to h)}{\mathcal{B}(J/\psi\to h)} \approx 0.128$. However, Chao *et al.* [15] argue that this ratio should be $\frac{\mathcal{B}(\eta_c(2S)\to h)}{\mathcal{B}(\eta_c(1S)\to h)} \approx 1$, or $1/2$ if there is a mixture with a glueball. Using known branching fractions of $\eta_c(2S)$ and $\eta_c(1S)$, a global fit is performed and experimental results are found to be significantly different from the above theoretical predictions [16].

In this paper, using $(27.12 \pm 0.14) \times 10^8$ $\psi(2S)$ events collected by the BESIII detector in 2009, 2012, and 2021 [17], the decay $\eta_c(2S) \to p\bar{p}$ is searched for through the radiative transition $\psi(2S) \to \gamma\eta_c(2S)$. However, no significant signal is observed. With the same analysis strategy, the branching fractions of $\chi_{cJ} \to p\bar{p}$ $(J = 0, 1, 2)$ are determined with improved precision.

II. BESIII DETECTOR AND MONTE CARLO SIMULATION

The BESIII detector [18] records symmetric e^+e^- collisions provided by the BEPCII storage ring [19] in

[*]Full author list given at the end of the article.

the center-of-mass energy ranging from 1.85 to 4.95 GeV, with a peak luminosity of 1.1×10^{33} cm^{-2} s^{-1} achieved at $\sqrt{s} = 3.773$ GeV. BESIII has collected large data samples in this energy region [20]. The cylindrical core of the BESIII detector covers 93% of the full solid angle and consists of a helium-based multilayer drift chamber (MDC), a time-of-flight system (TOF), and a CsI(Tl) electromagnetic calorimeter (EMC), which are all enclosed in a superconducting solenoidal magnet providing a 1.0 T magnetic field. The solenoid is supported by an octagonal flux-return yoke with resistive plate counter muon identification modules interleaved with steel. The charged-particle momentum resolution at 1 GeV/c is 0.5%, and the resolution of the specific ionization energy (dE/dx) is 6% for electrons from Bhabha scattering. The EMC measures photon energies with a resolution of 2.5% (5%) at 1 GeV in the barrel (end-cap) region. The time resolution in the TOF plastic scintillator barrel region is 68 ps, while that in the end-cap region was 110 ps. The end-cap TOF system was upgraded in 2015 using multigap resistive plate chamber technology, providing a time resolution of 60 ps, which benefits 85% of the data used in this analysis [21].

Monte Carlo (MC) simulated samples produced with GEANT4-based [22] software, which includes the geometric description of the BESIII detector and the detector response, are used to determine detection efficiencies and to estimate backgrounds. The simulation models the beam energy spread and initial state radiation (ISR) in the e^+e^- annihilations with the generator KKMC [23]. The inclusive MC sample includes the production of the $\psi(2S)$ resonance, the ISR production of the J/ψ, and the continuum processes incorporated in KKMC [23]. Known decay modes are modeled with EVTGEN [24,25] using branching fractions taken from the Particle Data Group (PDG) [10]. The remaining unknown charmonium decays are modeled with LUNDCHARM [26,27]. Final state radiation (FSR) from charged final state particles is incorporated using PHOTOS [28]. Exclusive MC samples are generated to determine the detection efficiency and optimize selection criteria. The process of $\psi(2S) \to \gamma\chi_{cJ}/\eta_c(2S)$ is generated following the angular distribution of $(1 + \lambda\cos^2\theta_1)$, where θ_1 is the polar angle of the radiative photon in the rest frame of $\psi(2S)$ and the value of λ is set to be 1 for $\eta_c(2S)$ and 1, $-1/3$, $1/13$ for χ_{cJ} $(J = 0, 1, 2)$, respectively [29]. The $\chi_{cJ} \to p\bar{p}$ decays are generated with $(1 + \alpha\cos^2\theta_2)$ distribution, where θ_2 is the polar angle of proton in the χ_{cJ} helicity frame and α is determined from data. The $\eta_c(2S) \to p\bar{p}$ decay is generated with a phase-space (PHSP) model.

III. EVENT SELECTION

The final state of interest contains two charged particles and one neutral particle. Charged tracks detected in the MDC are required to be within a polar angle (θ) range of $|\cos\theta| < 0.93$, where θ is defined with respect to the z axis, the symmetry axis of the MDC. The distance of the closest approach to the interaction point (IP) must be less than 10 cm along the z axis, $|V_z|$, and less than 1 cm in the transverse plane, $|V_{xy}|$. Two good charged tracks are required in the final state, and the total charge must be equal to zero.

The particle identification (PID) for charged tracks combines measurements of the dE/dx in the MDC and the flight time in the TOF to form likelihoods $\mathcal{L}(h)$ ($h = p$, K, π) for each hadron (h) hypothesis. A charged track is identified as a proton when the proton hypothesis has the maximum likelihood value, i.e. $\mathcal{L}(p) > \mathcal{L}(K)$ and $\mathcal{L}(p) > \mathcal{L}(\pi)$. The two good charged tracks must be identified as a proton and an antiproton.

In the selection of good photon candidates, the deposited energy for a cluster is required to be larger than 25 MeV in both the barrel ($|\cos\theta| < 0.80$) and end-cap ($0.86 < |\cos\theta| < 0.92$) regions. To suppress electronic noise and unrelated showers, the difference between the EMC time and the event start time is required to be within [0, 700] ns. The opening angle between the cluster and the closest good charged track is required to be larger than 20° for a proton and 30° for an antiproton. The number of good photon candidates is required to be greater than zero.

A vertex fit of the two charged tracks is performed to check if they are consistent with coming from the IP. Next, a four-constraint (4C) kinematic fit [30] is performed with all the final state particles, where the summed four-momentum of two charged tracks and a neutral track is constrained to the initial four-momentum of $\psi(2S)$. For the events with more than one photon candidate, the photon with the minimum $\chi^2_{\rm 4C}$ value is selected. The $\chi^2_{\rm 4C}$ is required to be less than 60, which is optimized by maximizing the figure of merit defined as $S/\sqrt{S+B}$, where S and B are the expected yields of signal and background events in the $\eta_c(2S)$ signal region normalized to data. S is estimated by $N^{\rm tot}_{\psi(2S)} \times \mathcal{B}(\psi(2S) \to \gamma\eta_c(2S)) \times \mathcal{B}(\eta_c(2S) \to p\bar{p}) \times \epsilon^{\rm MC}$, where $N^{\rm tot}_{\psi(2S)}$ is the number of $\psi(2S)$ events, $\mathcal{B}(\psi(2S) \to \gamma\eta_c(2S))$ is taken from PDG [10], $\mathcal{B}(\eta_c(2S) \to p\bar{p})$ is set to the LHCb measurement [12], and $\epsilon^{\rm MC}$ is the detection efficiency. B is the number of background events estimated from the inclusive MC sample.

IV. BACKGROUND ANALYSIS

The inclusive MC sample shows that the main backgrounds are from $\psi(2S) \to \gamma p\bar{p}$, $p\bar{p}$, and $\pi^0 p\bar{p}$ processes. The other backgrounds account for only 1% of all the background events, which is thereby negligible, and there is no peaking background. The nonresonant $\psi(2S) \to \gamma p\bar{p}$ background shares the same final state as the signal channel and therefore cannot be suppressed. The other two backgrounds $\psi(2S) \to p\bar{p}$ and $\psi(2S) \to \pi^0 p\bar{p}$, which have one less or one more photon, respectively, as well as the

contribution from the continuum production will be discussed in detail below.

A. Background of $\psi(2S) \to p\bar{p}$

Events of $\psi(2S) \to p\bar{p}$ accompanied by a fake photon or a FSR photon can easily pass through the event selection. For the events with a fake photon, the four-momentum of the proton and antiproton is expected to equal to that of $\psi(2S)$. Based on this, a three-constraint (3C) kinematic fit is performed where the momentum magnitude of the photon is allowed to float. Figure 1 shows the $M_{p\bar{p}}$ distributions from $\psi(2S) \to \gamma\eta_c(2S), \eta_c(2S) \to p\bar{p}$, and $\psi(2S) \to p\bar{p}$ MC samples after 4C and 3C kinematic fits. The peak of $\psi(2S) \to p\bar{p}$ is significantly separated from the $\eta_c(2S)$ signal after the 3C kinematic fit. Therefore, the $M^{3C}_{p\bar{p}}$ distribution is used to determine the signal yield. In addition, $\chi^2_{4C}(\gamma p\bar{p}) < \chi^2_{4C}(p\bar{p})$ is required to further suppress the background.

The consistency of the FSR photon between MC simulation and data has been checked using the control sample $J/\psi \to p\bar{p}\gamma_{\rm FSR}$. With the same proton and antiproton selection criteria as for our signal, the selected numbers of events with a FSR photon are 3307 ± 58 in data and 3200 ± 57 in MC, which are consistent with each other within the statistical uncertainty. Thus, we use the MC simulation to describe the FSR contribution in our fit process directly.

B. Background of $\psi(2S) \to \pi^0 p\bar{p}$

The process of $\psi(2S) \to \pi^0 p\bar{p}$ can contaminate our signal if a soft photon is not detected. To estimate this contribution, we generate corresponding MC samples based on partial wave analysis results [31]. After the event selection, the distribution of $M^{3C}_{p\bar{p}}$, which is described by a Novosibirsk function [32], is shown in Fig. 2. There are two solutions for the branching fraction of $\psi(2S) \to \pi^0 p\bar{p}$ due to the interference between the resonance and continuum production, which are $(133.9 \pm 11.2 \pm 2.3) \times 10^{-6}$ for constructive interference and $(183.7 \pm 13.7 \pm 3.2) \times 10^{-6}$ for destructive interference. We choose the second one as the nominal value to estimate the number of background events because it is more consistent with results from a data-driven method.

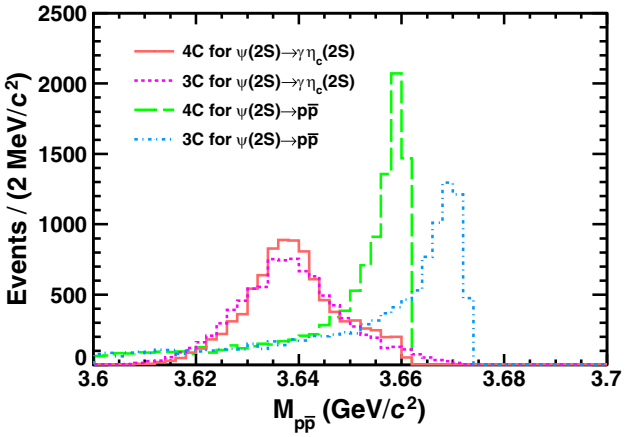

FIG. 1. The $M_{p\bar{p}}$ distributions for $\psi(2S) \to \gamma\eta_c(2S), \eta_c(2S) \to p\bar{p}$ MC events with 4C (red solid line) and 3C (purple dashed line) kinematic fits, and $\psi(2S) \to p\bar{p}$ MC events with 4C (green dashed line) and 3C (blue dash-dotted line) kinematic fits. The sharp cutoffs of the green and blue histograms are due to the photon energy threshold of 25 MeV.

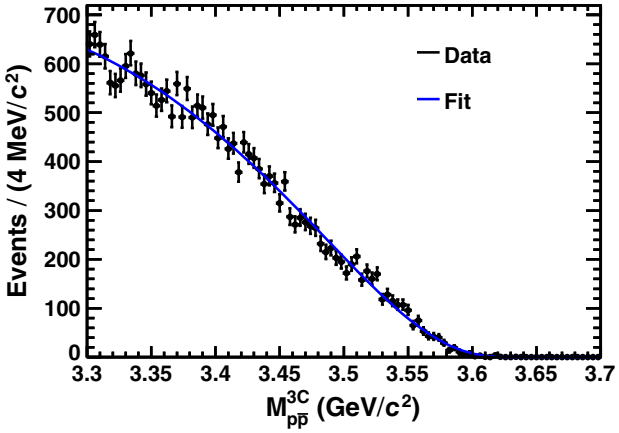

FIG. 2. The $M^{3C}_{p\bar{p}}$ distribution. The black dots with error bars are the MC simulated $\psi(2S) \to \pi^0 p\bar{p}$ events. The blue solid curve is the fit result with a Novosibirsk function.

C. Continuum background

The continuum production contribution is estimated with a data sample taken at $\sqrt{s} = 3.65$ GeV. Considering the energy difference between 3.65 and 3.686 GeV, the $M_{p\bar{p}}$ distribution is shifted according to the transformation $m \to a(m - m_0) + m_0$, where $m_0 = 1.877$ GeV/c^2 is the mass threshold of $p\bar{p}$ and the coefficient $a = (3.686 - m_0)/(3.65 - m_0) = 1.02$. The number of events is scaled based on the cross sections and luminosities at the two energy points. The resulting scale factor is calculated to be $f_{\rm continuum} = \frac{\mathcal{L}_{3.686}}{\mathcal{L}_{3.65}} \cdot (\frac{3.65}{3.686})^2 = 9.73$.

V. BRANCHING FRACTION MEASUREMENT

The signal yields are obtained by performing an unbinned maximum likelihood fit to the $M^{3C}_{p\bar{p}}$ distribution in the range of $[3.3, 3.7]$ GeV/c^2, which covers the $\eta_c(2S)$ and χ_{cJ} signal regions. The line shapes of $\eta_c(2S)$ and χ_{cJ} are described as

$$\left(E_\gamma^3 \times BW(m; m_0, \Gamma) \times f_d(E_\gamma) \times \epsilon(m)\right) \otimes \mathrm{DG}.$$

Here, m is $M^{3C}_{p\bar{p}}$, and the first term E_γ^3 is the PHSP factor, where E_γ is the energy of the transition photon in the rest frame of $\psi(2S)$, calculated as $E_\gamma = (m^2_{\psi(2S)} - m^2)/(2m_{\psi(2S)})$,

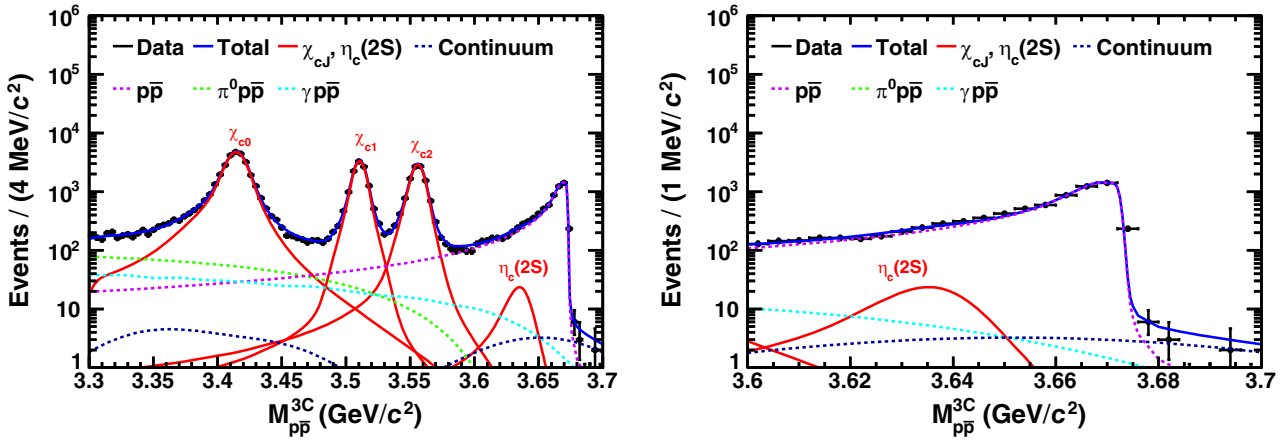

FIG. 3. The $M^{3C}_{p\bar{p}}$ distribution and fit result in the full fit range (left) and the $\eta_c(2S)$ signal region (right). The black dots with error bars are data, and the blue solid curve is the total fit. The four red solid lines are the χ_{c0}, χ_{c1}, χ_{c2}, and $\eta_c(2S)$ signals. The purple, green, cyan, and dark blue dashed lines show the background shapes of $\psi(2S) \to p\bar{p}(\gamma_{\rm FSR})$, $\psi(2S) \to \pi^0 p\bar{p}$, $\psi(2S) \to \gamma p\bar{p}$, and the continuum production, respectively.

with $m_{\psi(2S)}$ being the mass of $\psi(2S)$ [10]. $BW(m; m_0, \Gamma)$ is the Breit-Wigner function, with m_0 and Γ as the masses and widths of $\eta_c(2S)$ and χ_{cJ} [10]. $f_d(E_\gamma)$ is a damping factor used to suppress the divergence in the lower side of the mass spectrum. The form of the damping function used in the nominal fit, proposed by the KEDR Collaboration [33], is taken as $\frac{E_0^2}{E_\gamma E_0 + (E_\gamma - E_0)^2}$, where $E_0 = \frac{m^2_{\psi(2S)} - m^2_{\eta_c(2S)}}{2m_{\psi(2S)}}$ is the most probable energy of the transition photon. The efficiency curve $\epsilon(m)$ is based on the PHSP MC sample. We divide the $M^{3C}_{p\bar{p}}$ distribution into 40 bins, calculate the efficiency for each bin, and fit these efficiencies to obtain the curve. The detector resolution is modeled by a double-Gaussian (DG) function. For χ_{cJ} signals, the parameters of the DG function are free, while for the $\eta_c(2S)$ signal, the parameters are extrapolated from the χ_{c1} and χ_{c2} parameters with a first-order polynomial function and are fixed.

In the fitting process, four background components are considered. The line shape of $\psi(2S) \to p\bar{p}$ is modeled by a Crystal-Ball (CB) [34] function convolved with a DG function. The parameters of the CB function are fixed based on MC simulation, while the parameters of the DG function are floated. The background from $\psi(2S) \to \pi^0 p\bar{p}$ is described by a Novosibirsk function, with the yield fixed at 3043 ± 55. The shape of the nonresonant $\psi(2S) \to \gamma p\bar{p}$ process is determined by MC simulation, and its magnitude is fixed at 2001 ± 45 according to the PDG branching fraction [10]. Additionally, the line shape of the continuum production is fixed, and the number of events is 243 ± 16.

Figure 3 shows the $M^{3C}_{p\bar{p}}$ distribution after event selection and the fit results. The left panel shows the full fit range, while the right panel focuses on the $\eta_c(2S)$ signal region. The goodness of fit is $\chi^2/{\rm ndf} = 39.25/25 = 1.57$, where ndf is the number of degrees of freedom. The branching fractions of $\chi_{cJ} \to p\bar{p}$ are calculated by

$$\mathcal{B}(\chi_{cJ} \to p\bar{p}) = \frac{N^{\rm obs}_{\rm J}}{N^{\rm tot}_{\psi(2S)} \times \mathcal{B}(\psi(2S) \to \gamma\chi_{cJ}) \times \epsilon^{\rm MC}_{\rm J}},$$

where $N^{\rm obs}_{\rm J}$ are the signal yields from the fit, $\mathcal{B}(\psi(2S) \to \gamma\chi_{cJ})$ are taken from PDG [10], and $\epsilon^{\rm MC}_{\rm J}$ are the detection efficiencies. The signal yields, detection efficiencies, and the corresponding numerical results are listed in Table I.

The statistical significance of the $\eta_c(2S)$ signal is estimated to be 2.5σ by comparing the likelihood values with and without the signal component. The detection efficiency for $\eta_c(2S) \to p\bar{p}$ is $(45.5 \pm 0.2)\%$, and the signal yield is 158 ± 63. Dividing by $\mathcal{B}(\psi(2S) \to \gamma\eta_c(2S))$ [35], the branching fraction $\mathcal{B}(\eta_c(2S) \to p\bar{p})$ is determined to be $(2.46 \pm 0.98) \times 10^{-4}$, where the uncertainty is statistical. Using a Bayesian method [36], the

TABLE I. Signal yields, detection efficiencies, and the measured branching fractions of $\chi_{cJ} \to p\bar{p}$, as well as the branching fractions from BESIII previous measurements [11] and the PDG [10]. Here the first uncertainties are statistical and the second systematic.

Channel	$N^{\rm obs}_{\rm J}$	$\epsilon^{\rm MC}_{\rm J}$ (%)	$\mathcal{B}$ (this work)	BESIII (2013)	PDG
$\chi_{c0} \to p\bar{p}$	31268 ± 189	47.0 ± 0.2	$(2.51 \pm 0.02 \pm 0.08) \times 10^{-4}$	$(2.45 \pm 0.08 \pm 0.13) \times 10^{-4}$	$(2.21 \pm 0.08) \times 10^{-4}$
$\chi_{c1} \to p\bar{p}$	11279 ± 119	52.2 ± 0.2	$(8.16 \pm 0.09 \pm 0.25) \times 10^{-5}$	$(8.6 \pm 0.5 \pm 0.5) \times 10^{-5}$	$(7.60 \pm 0.34) \times 10^{-5}$
$\chi_{c2} \to p\bar{p}$	10672 ± 115	49.6 ± 0.2	$(8.33 \pm 0.09 \pm 0.22) \times 10^{-5}$	$(8.4 \pm 0.5 \pm 0.5) \times 10^{-5}$	$(7.33 \pm 0.33) \times 10^{-5}$

TABLE II. Relative systematic uncertainties (in %) in the branching fraction measurements of $\chi_{cJ} \to p\bar{p}$ $(J = 0, 1, 2)$ and the search for $\eta_c(2S) \to p\bar{p}$.

Source	$\chi_{c0} \to p\bar{p}$	$\chi_{c1} \to p\bar{p}$	$\chi_{c2} \to p\bar{p}$	$\eta_c(2S) \to p\bar{p}$
Tracking	1.10	0.96	0.91	0.8
PID	0.96	0.99	1.10	1.7
Photon reconstruction	0.50	0.50	0.50	1.0
Kinematic fit	0.11	0.10	0.10	0.2
Generator model	0.21	0.19	0.20	6.8
Number of $\psi(2S)$ events	0.52	0.52	0.52	0.5
Quoted branching fractions	2.04	2.46	2.10	38.5
Form of damping function	0.00	0.01	0.12	10.1
Efficiency curve	0.02	0.02	0.04	1.3
DG parameters	0.00	0.02	0.00	14.6
Shape of $\psi(2S) \to \pi^0 p\bar{p}$ background	0.03	0.05	0.00	0.6
Number of $\psi(2S) \to \pi^0 p\bar{p}$ background events	1.85	0.79	0.15	6.3
Number of $\psi(2S) \to \gamma p\bar{p}$ background events	0.79	0.53	0.34	3.8
Number of continuum background events	0.03	0.02	0.01	0.6
Total	3.30	3.07	2.68	41.2

upper limit of the product branching fraction at 90% CL is determined to be

$$\mathcal{B}\big(\psi(2S) \to \gamma\eta_c(2S)\big) \times \mathcal{B}\big(\eta_c(2S) \to p\bar{p}\big) < 2.2 \times 10^{-7}.$$

VI. SYSTEMATIC UNCERTAINTIES

The systematic uncertainties in the branching fraction measurements are listed in Table II. The systematic uncertainties are divided into two parts: the multiplicative and additive terms. The multiplicative uncertainties include tracking, PID, photon reconstruction, kinematic fit, generator model, and number of $\psi(2S)$ events. The additive uncertainties are those related to the fit process, including the form of the damping function, efficiency curve, DG parameters, number of $\gamma p\bar{p}$ background events, shape and size of $\pi^0 p\bar{p}$ background, and number of continuum background events. The total systematic uncertainty is obtained by summing all contributions in quadrature, assuming they are independent.

To determine the uncertainties of tracking and PID for the proton, the uncertainties, given by the efficiency differences between data and MC control samples as a function of transverse momentum, are reweighted according to the transverse momentum distributions of the proton and antiproton. To cover the momentum range of p and $\bar{p}$, the control samples $J/\psi \to p\bar{p}$ and $e^+e^- \to p\bar{p}$ are used. The uncertainties of tracking are 1.10%, 0.96%, 0.91%, and 0.82%, while the uncertainties due to PID are 0.96%, 0.99%, 1.10%, and 1.65% for the $\chi_{c0,1,2}$ and $\eta_c(2S)$ decays, respectively.

The uncertainty of photon reconstruction for χ_{cJ} decays in both the barrel and end-cap regions is determined to be 0.5%, using a control sample $e^+e^- \to \gamma\mu^+\mu^-$. The energy of transition photon from $\psi(2S) \to \gamma\eta_c(2S)$ is less than 0.1 GeV, and the systematic uncertainty is assigned to be 1% by using the control samples $J/\psi \to \rho^0\pi^0$ and $e^+e^- \to \gamma\gamma$ [37].

To estimate the uncertainty introduced by the kinematic fit, the helix parameters are corrected in the MC simulation to reduce the difference between data and MC events [11]. The uncertainties of the kinematic fit are taken as half of the efficiency differences before and after the helix parameter correction, which are 0.11%, 0.10%, 0.10%, and 0.22% for $\chi_{c0,1,2}$ and $\eta_c(2S)$ decays, respectively.

The helicity angular distributions of the proton in the χ_{cJ} signal region are measured from data and described by $1 + \alpha\cos^2\theta_2$ [11]. The $\chi_{cJ} \to p\bar{p}$ decays are simulated with this α value in the MC sample. By varying the α value by $\pm 1\sigma$, the maximum difference of MC efficiencies is taken as the uncertainty of the generator model. For the process of $\eta_c(2S) \to p\bar{p}$, the uncertainty is estimated by taking $\alpha = 1$ and -1.

The systematic uncertainty of the efficiency curve $\epsilon(m)$ is estimated by changing the number of bins to 20, 30, 60, 80, 100, 150, and 200. The maximum difference in the branching fractions from these efficiency curves is taken as the uncertainty. The uncertainty caused by the form of damping function is estimated by changing it to $\exp(-E_\gamma^2/8\beta^2)$, as used by the CLEO Collaboration [38]. The parameter β is free for χ_{cJ} signal and fixed at 65 MeV for the $\eta_c(2S)$ signal. The uncertainty of the $\eta_c(2S)$ DG parameters is estimated using an alternative set, where the parameters are the same as the χ_{c2} signal.

Instead of the Novosibirsk function, an ARGUS function [39] is used to describe the shape of the $\psi(2S) \to \pi^0 p\bar{p}$ background, and the uncertainty in the number of $\psi(2S) \to \pi^0 p\bar{p}$ events is determined by the difference in signal yield

compared to the nominal value. For the number of other background events, including nonresonant and continuum processes, we change them by $\pm 1\sigma$, and the maximum difference of the signal yield is taken as the uncertainty.

The number of $\psi(2S)$ events is determined to be $(27.12 \pm 0.14) \times 10^8$ [17], and its uncertainty of 0.52% is taken as a systematic uncertainty. The branching fractions of $\psi(2S) \to \gamma\chi_{cJ}(J = 0, 1, 2)$ are $(9.79 \pm 0.20)\%$, $(9.75 \pm 0.24)\%$, and $(9.52 \pm 0.20)\%$ [10], corresponding to the uncertainties of 2.04%, 2.46%, and 2.10%, respectively. The branching fraction of $\psi(2S) \to \gamma\eta_c(2S)$ is $(5.2 \pm 0.3(\text{stat}) \pm 0.5(\text{syst})^{+1.9}_{-1.4}(\text{extr})) \times 10^{-4}$ [35], corresponding to a 38% uncertainty.

With fit-related uncertainties considered, the final significance for $\eta_c(2S)$ is conservatively estimated to be 1.7σ. It is the DG function that yields the largest upper limit among the additive uncertainties. The red solid line in Fig. 4 shows the normalized likelihood distribution. This distribution convolved with a Gaussian function, shown by the blue dashed line, shows the effect of multiplicative uncertainty. This process can be described as

$$L'(x) = \int_0^1 L(x; N_{\text{sig}}\epsilon/\hat{\epsilon}) \exp\left[-\frac{(\epsilon - \hat{\epsilon})}{2\sigma_s^2}\right] d\epsilon,$$

where $L(x; N_{\text{sig}}\epsilon/\hat{\epsilon})$ and $L'(x)$ are the likelihood distributions before and after incorporating the multiplicative systematic uncertainty, respectively, $\hat{\epsilon}$ is the nominal detection efficiency, and σ_s is the total multiplicative systematic uncertainty, which is 7.15% obtained from Table II. Taking the systematic uncertainty into account, the upper limit at the 90% CL of the product branching fraction is 2.4×10^{-7}.

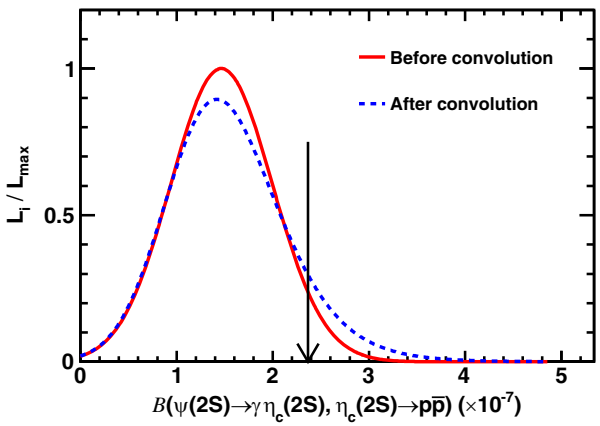

FIG. 4. The red solid line represents the normalized likelihood distribution incorporating the additive systematic uncertainty, while the blue dashed line further includes the multiplicative systematic uncertainty. The black arrow indicates the upper limit of the product branching fraction at the 90% CL.

VII. SUMMARY

Using $(27.12 \pm 0.14) \times 10^8$ $\psi(2S)$ events collected by the BESIII detector, we search for the decay $\eta_c(2S) \to p\bar{p}$. A signal with significance of only 1.7σ is observed. The upper limit of the product branching fraction at the 90% CL is determined to be 2.4×10^{-7}, which is reduced by an order of magnitude compared to the previous BESIII measurements. Dividing by the branching fraction of $\psi(2S) \to \gamma\eta_c(2S)$ [35], the upper limit of the branching fraction of $\eta_c(2S) \to p\bar{p}$ is calculated to be $\mathcal{B}(\eta_c(2S) \to p\bar{p}) < 7.5 \times 10^{-4}$. This result is consistent with the previous result from the LHCb Collaboration, $\mathcal{B}(\eta_c(2S) \to p\bar{p}) = (7.89 \pm 2.43 \pm 1.89) \times 10^{-5}$ [12]. Additionally, the ratio $\mathcal{B}(\eta_c(2S) \to p\bar{p})/\mathcal{B}(\eta_c(2S) \to K\bar{K}\pi)$ is calculated to be less than 2.7×10^{-2} at the 90% CL. This calculation is based on the previous BESIII measurement of $\mathcal{B}(\psi(2S) \to \gamma\eta_c(2S)) \times \mathcal{B}(\eta_c(2S) \to K\bar{K}\pi)$ [35], with common systematic uncertainties effectively canceled.

The branching fractions of $\chi_{cJ} \to p\bar{p}$ are also measured with improved precision and listed in Table I, where the first uncertainties are statistical and the second systematic. Our results deviate from the PDG [10] values by 2.7σ for χ_{c0} and 2.4σ for χ_{c2} but are consistent with the previous BESIII measurement [11]. The data used in this analysis incorporate the data from the earlier study. Therefore, this measurement supersedes that reported in Ref. [11].

ACKNOWLEDGMENTS

The BESIII Collaboration thanks the staff of BEPCII and the IHEP computing center for their strong support. This work is supported in part by National Key R&D Program of China under Contracts No. 2020YFA0406300, No. 2020YFA0406400, and No. 2023YFA1606000; National Natural Science Foundation of China (NSFC) under Contracts No. 12275058, No. 12375070, No. 11635010, No. 11735014, No. 11935015, No. 11935016, No. 11935018, No. 12025502, No. 12035009, No. 12035013, No. 12061131003, No. 12192260, No. 12192261, No. 12192262, No. 12192263, No. 12192264, No. 12192265, No. 12221005, No. 12225509, No. 12235017, and No. 12361141819; the Chinese Academy of Sciences (CAS) Large-Scale Scientific Facility Program; the CAS Center for Excellence in Particle Physics (CCEPP); Joint Large-Scale Scientific Facility Funds of the NSFC and CAS under Contract No. U1832207; 100 Talents Program of CAS; The Institute of Nuclear and Particle Physics (INPAC) and Shanghai Key Laboratory for Particle Physics and Cosmology; German Research Foundation DFG under Contracts No. FOR5327 and No. GRK 2149; Istituto Nazionale di Fisica Nucleare, Italy; Knut and Alice Wallenberg Foundation under Contracts No. 2021.0174 and No. 2021.0299; Ministry of Development of Turkey

under Contract No. DPT2006K-120470; National Research Foundation of Korea under Contract No. NRF-2022R1A2C1092335; National Science and Technology fund of Mongolia; National Science Research and Innovation Fund (NSRF) via the Program Management Unit for Human Resources & Institutional Development, Research and Innovation of Thailand under Contracts No. B16F640076 and No. B50G670107; Polish National Science Centre under Contract No. 2019/35/O/ST2/02907; Swedish Research Council under Contract No. 2019.04595; The Swedish Foundation for International Cooperation in Research and Higher Education under Contract No. CH2018-7756; and U.S. Department of Energy under Contract No. DE-FG02-05ER41374.

DATA AVAILABILITY

The data that support the findings of this article are not publicly available. The data are available from the authors upon reasonable request.

[1] J. J. Aubert *et al.* (E598 Collaboration), Phys. Rev. Lett. **33**, 1404 (1974).
[2] J. E. Augustin *et al.* (SLAC-SP-017 Collaboration), Phys. Rev. Lett. **33**, 1406 (1974).
[3] C. Bacci *et al.*, Phys. Rev. Lett. **33**, 1408 (1974).
[4] S. K. Choi *et al.* (Belle Collaboration), Phys. Rev. Lett. **89**, 102001 (2002).
[5] D. M. Asner *et al.* (CLEO Collaboration), Phys. Rev. Lett. **92**, 142001 (2004).
[6] B. Aubert *et al.* (*BABAR* Collaboration), Phys. Rev. Lett. **92**, 142002 (2004).
[7] B. Aubert *et al.* (*BABAR* Collaboration), Phys. Rev. D **72**, 031101 (2005).
[8] K. Abe *et al.* (Belle Collaboration), Phys. Rev. Lett. **98**, 082001 (2007).
[9] M. Ablikim *et al.* (BESIII Collaboration), Phys. Rev. Lett. **109**, 042003 (2012).
[10] S. Navas *et al.* (Particle Data Group), Phys. Rev. D **110**, 030001 (2024).
[11] M. Ablikim *et al.* (BESIII Collaboration), Phys. Rev. D **88**, 112001 (2013).
[12] R. Aaij *et al.* (LHCb Collaboration), Phys. Lett. B **769**, 305 (2017).
[13] S. J. Brodsky and G. P. Lepage, Phys. Rev. D **24**, 2848 (1981).
[14] M. Anselmino, M. Genovese, and E. Predazzi, Phys. Rev. D **44**, 1597 (1991).
[15] K. T. Chao, Y. F. Gu, and S. F. Tuan, Commun. Theor. Phys. **25**, 471 (1996).
[16] H. P. Wang and C. Z. Yuan, Chin. Phys. C **46**, 071001 (2022).
[17] M. Ablikim *et al.* (BESIII Collaboration), Chin. Phys. C **48**, 093001 (2024).
[18] M. Ablikim *et al.* (BESIII Collaboration), Nucl. Instrum. Methods Phys. Res., Sect. A **614**, 345 (2010).
[19] C. H. Yu *et al.*, *Proceedings of IPAC2016, Busan, Korea* (2016), 10.18429/JACoW-IPAC2016-TUYA01.
[20] M. Ablikim *et al.* (BESIII Collaboration), Chin. Phys. C **44**, 040001 (2020).
[21] X. Li *et al.*, Radiat. Detect. Technol. Methods **1**, 13 (2017); Y. X. Guo *et al.*, Radiat. Detect. Technol. Methods **1**, 15 (2017); P. Cao *et al.*, Nucl. Instrum. Methods Phys. Res., Sect. A **953**, 163053 (2020).
[22] S. Agostinelli *et al.* (GEANT4 Collaboration), Nucl. Instrum. Methods Phys. Res., Sect. A **506**, 250 (2003).
[23] S. Jadach, B. F. L. Ward, and Z. Was, Comput. Phys. Commun. **130**, 260 (2000); Phys. Rev. D **63**, 113009 (2001).
[24] D. J. Lange, Nucl. Instrum. Methods Phys. Res., Sect. A **462**, 152 (2001).
[25] R. G. Ping, Chin. Phys. C **32**, 599 (2008).
[26] J. C. Chen, G. S. Huang, X. R. Qi, D. H. Zhang, and Y. S. Zhu, Phys. Rev. D **62**, 034003 (2000).
[27] R. L. Yang, R. G. Ping, and H. Chen, Chin. Phys. Lett. **31**, 061301 (2014).
[28] E. Barberio, B. van Eijk, and Z. Was, Comput. Phys. Commun. **66**, 115 (1991).
[29] W. M. Tanenbaum *et al.*, Phys. Rev. D **17**, 1731 (1978).
[30] L. Yan *et al.*, Chin. Phys. C **34**, 204 (2010).
[31] M. Ablikim *et al.* (BESIII Collaboration), Partial wave analyses of $\psi(2S) \to p\bar{p}\pi^0$ and $\psi(2S) \to p\bar{p}\eta$ (to be published).
[32] H. S. Ahn *et al.*, Nucl. Instrum. Methods Phys. Res., Sect. A **410**, 179 (1998).
[33] V. M. Malyshev (KEDR collaboration), Int. J. Mod. Phys. Conf. Ser. **02**, 188 (2011).
[34] S. Chatrchyan *et al.* (CMS Collaboration), Phys. Rev. D **89**, 092007 (2014).
[35] M. Ablikim *et al.* (BESIII Collaboration), Phys. Rev. D **109**, 032004 (2024).
[36] J. Conrad, O. Botner, A. Hallgren, and C. Pérez de los Heros, Phys. Rev. D **67**, 012002 (2003).
[37] M. Ablikim *et al.* (BESIII Collaboration), Phys. Rev. D **81**, 052005 (2010).
[38] R. E. Mitchell *et al.* (CLEO Collaboration), Phys. Rev. Lett. **102**, 011801 (2009).
[39] H. Albrecht *et al.* (ARGUS Collaboration), Phys. Lett. B **241**, 278 (1990).

M. Ablikim,[1] M. N. Achasov,[4,c] P. Adlarson,[76] O. Afedulidis,[3] X. C. Ai,[81] R. Aliberti,[35] A. Amoroso,[75a,75c] Y. Bai,[57] O. Bakina,[36] I. Balossino,[29a] Y. Ban,[46,h] H.-R. Bao,[64] V. Batozskaya,[1,44] K. Begzsuren,[32] N. Berger,[35] M. Berlowski,[44] M. Bertani,[28a] D. Bettoni,[29a] F. Bianchi,[75a,75c] E. Bianco,[75a,75c] A. Bortone,[75a,75c] I. Boyko,[36] R. A. Briere,[5] A. Brueggemann,[69] H. Cai,[77] X. Cai,[1,58] A. Calcaterra,[28a] G. F. Cao,[1,64] N. Cao,[1,64] S. A. Cetin,[62a] X. Y. Chai,[46,h] J. F. Chang,[1,58] G. R. Che,[43] Y. Z. Che,[1,58,64] G. Chelkov,[36,b] C. Chen,[43] C. H. Chen,[9] Chao Chen,[55] G. Chen,[1] H. S. Chen,[1,64] H. Y. Chen,[20] M. L. Chen,[1,58,64] S. J. Chen,[42] S. L. Chen,[45] S. M. Chen,[61] T. Chen,[1,64] X. R. Chen,[31,64] X. T. Chen,[1,64] Y. B. Chen,[1,58] Y. Q. Chen,[34] Z. J. Chen,[25,i] S. K. Choi,[10] G. Cibinetto,[29a] F. Cossio,[75c] J. J. Cui,[50] H. L. Dai,[1,58] J. P. Dai,[79] A. Dbeyssi,[18] R. E. de Boer,[3] D. Dedovich,[36] C. Q. Deng,[73] Z. Y. Deng,[1] A. Denig,[35] I. Denysenko,[36] M. Destefanis,[75a,75c] F. De Mori,[75a,75c] B. Ding,[67,1] X. X. Ding,[46,h] Y. Ding,[34] Y. Ding,[40] J. Dong,[1,58] L. Y. Dong,[1,64] M. Y. Dong,[1,58,64] X. Dong,[77] M. C. Du,[1] S. X. Du,[81] Y. Y. Duan,[55] Z. H. Duan,[42] P. Egorov,[36,b] G. F. Fan,[42] J. J. Fan,[19] Y. H. Fan,[45] J. Fang,[59] J. Fang,[1,58] S. S. Fang,[1,64] W. X. Fang,[1] Y. Q. Fang,[1,58] R. Farinelli,[29a] L. Fava,[75b,75c] F. Feldbauer,[3] G. Felici,[28a] C. Q. Feng,[72,58] J. H. Feng,[59] Y. T. Feng,[72,58] M. Fritsch,[3] C. D. Fu,[1] J. L. Fu,[64] Y. W. Fu,[1,64] H. Gao,[64] X. B. Gao,[41] Y. N. Gao,[46,h] Y. N. Gao,[19] Yang Gao,[72,58] S. Garbolino,[75c] I. Garzia,[29a,29b] P. T. Ge,[19] Z. W. Ge,[42] C. Geng,[59] E. M. Gersabeck,[68] A. Gilman,[70] K. Goetzen,[13] L. Gong,[40] W. X. Gong,[1,58] W. Gradl,[35] S. Gramigna,[29a,29b] M. Greco,[75a,75c] M. H. Gu,[1,58] Y. T. Gu,[15] C. Y. Guan,[1,64] A. Q. Guo,[31,64] L. B. Guo,[41] M. J. Guo,[50] R. P. Guo,[49] Y. P. Guo,[12,g] A. Guskov,[36,b] J. Gutierrez,[27] K. L. Han,[64] T. T. Han,[1] F. Hanisch,[3] X. Q. Hao,[19] F. A. Harris,[66] K. K. He,[55] K. L. He,[1,64] F. H. Heinsius,[3] C. H. Heinz,[35] Y. K. Heng,[1,58,64] C. Herold,[60] T. Holtmann,[3] P. C. Hong,[34] G. Y. Hou,[1,64] X. T. Hou,[1,64] Y. R. Hou,[64] Z. L. Hou,[1] B. Y. Hu,[59] H. M. Hu,[1,64] J. F. Hu,[56,j] Q. P. Hu,[72,58] S. L. Hu,[12,g] T. Hu,[1,58,64] Y. Hu,[1] G. S. Huang,[72,58] K. X. Huang,[59] L. Q. Huang,[31,64] P. Huang,[42] X. T. Huang,[50] Y. P. Huang,[1] Y. S. Huang,[59] T. Hussain,[74] F. Hölzken,[3] N. Hüsken,[35] N. in der Wiesche,[69] J. Jackson,[27] S. Janchiv,[32] Q. Ji,[1] Q. P. Ji,[19] W. Ji,[1,64] X. B. Ji,[1,64] X. L. Ji,[1,58] Y. Y. Ji,[50] X. Q. Jia,[50] Z. K. Jia,[72,58] D. Jiang,[1,64] H. B. Jiang,[77] P. C. Jiang,[46,h] S. S. Jiang,[39] T. J. Jiang,[16] X. S. Jiang,[1,58,64] Y. Jiang,[64] J. B. Jiao,[50] J. K. Jiao,[34] Z. Jiao,[23] S. Jin,[42] Y. Jin,[67] M. Q. Jing,[1,64] X. M. Jing,[64] T. Johansson,[76] S. Kabana,[33] N. Kalantar-Nayestanaki,[65] X. L. Kang,[9] X. S. Kang,[40] M. Kavatsyuk,[65] B. C. Ke,[81] V. Khachatryan,[27] A. Khoukaz,[69] R. Kiuchi,[1] O. B. Kolcu,[62a] B. Kopf,[3] M. Kuessner,[3] X. Kui,[1,64] N. Kumar,[26] A. Kupsc,[44,76] W. Kühn,[37] W. N. Lan,[19] T. T. Lei,[72,58] Z. H. Lei,[72,58] M. Lellmann,[35] T. Lenz,[35] C. Li,[47] C. Li,[43] C. H. Li,[39] Cheng Li,[72,58] D. M. Li,[81] F. Li,[1,58] G. Li,[1] H. B. Li,[1,64] H. J. Li,[19] H. N. Li,[56,j] Hui Li,[43] J. R. Li,[61] J. S. Li,[59] K. Li,[1] K. L. Li,[19] L. J. Li,[1,64] Lei Li,[48] M. H. Li,[43] P. L. Li,[64] P. R. Li,[38,k,l] Q. M. Li,[1,64] Q. X. Li,[50] R. Li,[17,31] T. Li,[50] T. Y. Li,[43] W. D. Li,[1,64] W. G. Li,[1,a] X. Li,[1,64] X. H. Li,[72,58] X. L. Li,[50] X. Y. Li,[1,8] X. Z. Li,[59] Y. Li,[19] Y. G. Li,[46,h] Z. J. Li,[59] Z. Y. Li,[79] C. Liang,[42] H. Liang,[72,58] Y. F. Liang,[54] Y. T. Liang,[31,64] G. R. Liao,[14] Y. P. Liao,[1,64] J. Libby,[26] A. Limphirat,[60] C. C. Lin,[55] C. X. Lin,[64] D. X. Lin,[31,64] T. Lin,[1] B. J. Liu,[1] B. X. Liu,[77] C. Liu,[34] C. X. Liu,[1] F. Liu,[1] F. H. Liu,[53] Feng Liu,[6] G. M. Liu,[56,j] H. Liu,[38,k,l] H. B. Liu,[15] H. H. Liu,[1] H. M. Liu,[1,64] Huihui Liu,[21] J. B. Liu,[72,58] K. Liu,[38,k,l] K. Y. Liu,[40] Ke Liu,[22] L. Liu,[72,58] L. C. Liu,[43] Lu Liu,[43] M. H. Liu,[12,g] P. L. Liu,[1] Q. Liu,[64] S. B. Liu,[72,58] T. Liu,[12,g] W. K. Liu,[43] W. M. Liu,[72,58] X. Liu,[39] X. Liu,[38,k,l] Y. Liu,[81] Y. Liu,[38,k,l] Y. B. Liu,[43] Z. A. Liu,[1,58,64] Z. D. Liu,[9] Z. Q. Liu,[50] X. C. Lou,[1,58,64] F. X. Lu,[59] H. J. Lu,[23] J. G. Lu,[1,58] Y. Lu,[7] Y. P. Lu,[1,58] Z. H. Lu,[1,64] C. L. Luo,[41] J. R. Luo,[59] M. X. Luo,[80] T. Luo,[12,g] X. L. Luo,[1,58] X. R. Lyu,[64] Y. F. Lyu,[43] F. C. Ma,[40] H. Ma,[79] H. L. Ma,[1] J. L. Ma,[1,64] L. L. Ma,[50] L. R. Ma,[67] Q. M. Ma,[1] R. Q. Ma,[1,64] R. Y. Ma,[19] T. Ma,[72,58] X. T. Ma,[1,64] X. Y. Ma,[1,58] Y. M. Ma,[31] F. E. Maas,[18] I. MacKay,[70] M. Maggiora,[75a,75c] S. Malde,[70] Y. J. Mao,[46,h] Z. P. Mao,[1] S. Marcello,[75a,75c] Y. H. Meng,[64] Z. X. Meng,[67] J. G. Messchendorp,[13,65] G. Mezzadri,[29a] H. Miao,[1,64] T. J. Min,[42] R. E. Mitchell,[27] X. H. Mo,[1,58,64] B. Moses,[27] N. Yu. Muchnoi,[4,c] J. Muskalla,[35] Y. Nefedov,[36] F. Nerling,[18,e] L. S. Nie,[20] I. B. Nikolaev,[4,c] Z. Ning,[1,58] S. Nisar,[11,m] Q. L. Niu,[38,k,l] W. D. Niu,[55] Y. Niu,[50] S. L. Olsen,[10,64] Q. Ouyang,[1,58,64] S. Pacetti,[28b,28c] X. Pan,[55] Y. Pan,[57] A. Pathak,[10] Y. P. Pei,[72,58] M. Pelizaeus,[3] H. P. Peng,[72,58] Y. Y. Peng,[38,k,l] K. Peters,[13,e] J. L. Ping,[41] R. G. Ping,[1,64] S. Plura,[35] V. Prasad,[33] F. Z. Qi,[1] H. R. Qi,[61] M. Qi,[42] S. Qian,[1,58] W. B. Qian,[64] C. F. Qiao,[64] J. H. Qiao,[19] J. J. Qin,[73] L. Q. Qin,[14] L. Y. Qin,[72,58] X. P. Qin,[12,g] X. S. Qin,[50] Z. H. Qin,[1,58] J. F. Qiu,[1] Z. H. Qu,[73] C. F. Redmer,[35] K. J. Ren,[39] A. Rivetti,[75c] M. Rolo,[75c] G. Rong,[1,64] Ch. Rosner,[18] M. Q. Ruan,[1,58] S. N. Ruan,[43] N. Salone,[44] A. Sarantsev,[36,d] Y. Schelhaas,[35] K. Schoenning,[76] M. Scodeggio,[29a] K. Y. Shan,[12,g] W. Shan,[24] X. Y. Shan,[72,58] Z. J. Shang,[38,k,l] J. F. Shangguan,[16] L. G. Shao,[1,64] M. Shao,[72,58] C. P. Shen,[12,g] H. F. Shen,[1,8] W. H. Shen,[64] X. Y. Shen,[1,64] B. A. Shi,[64] H. Shi,[72,58] J. L. Shi,[12,g] J. Y. Shi,[1] S. Y. Shi,[73] X. Shi,[1,58] J. J. Song,[19] T. Z. Song,[59] W. M. Song,[34,1] Y. J. Song,[12,g] Y. X. Song,[46,h,n] S. Sosio,[75a,75c] S. Spataro,[75a,75c] F. Stieler,[35] S. S. Su,[40] Y. J. Su,[64] G. B. Sun,[77] G. X. Sun,[1] H. Sun,[64] H. K. Sun,[1] J. F. Sun,[19] K. Sun,[61] L. Sun,[77] S. S. Sun,[1,64] T. Sun,[51,f] Y. J. Sun,[72,58] Y. Z. Sun,[1] Z. Q. Sun,[1,64] Z. T. Sun,[50] C. J. Tang,[54] G. Y. Tang,[1] J. Tang,[59] M. Tang,[72,58] Y. A. Tang,[77] L. Y. Tao,[73] M. Tat,[70] J. X. Teng,[72,58] V. Thoren,[76] W. H. Tian,[59] Y. Tian,[31,64] Z. F. Tian,[77] I. Uman,[62b] Y. Wan,[55] S. J. Wang,[50]

B. Wang,[1] Bo Wang,[72,58] C. Wang,[19] D. Y. Wang,[46,h] H. J. Wang,[38,k,l] J. J. Wang,[77] J. P. Wang,[50] K. Wang,[1,58] L. L. Wang,[1] L. W. Wang,[34] M. Wang,[50] N. Y. Wang,[64] S. Wang,[12,g] S. Wang,[38,k,l] T. Wang,[12,g] T. J. Wang,[43] W. Wang,[59] W. Wang,[73] W. P. Wang,[35,58,72,o] X. Wang,[46,h] X. F. Wang,[38,k,l] X. J. Wang,[39] X. L. Wang,[12,g] X. N. Wang,[1] Y. Wang,[61] Y. D. Wang,[45] Y. F. Wang,[1,58,64] Y. H. Wang,[38,k,l] Y. L. Wang,[19] Y. N. Wang,[45] Y. Q. Wang,[1] Yaqian Wang,[17] Yi Wang,[61] Z. Wang,[1,58] Z. L. Wang,[73] Z. Y. Wang,[1,64] D. H. Wei,[14] F. Weidner,[69] S. P. Wen,[1] Y. R. Wen,[39] U. Wiedner,[3] G. Wilkinson,[70] M. Wolke,[76] L. Wollenberg,[3] C. Wu,[39] J. F. Wu,[1,8] L. H. Wu,[1] L. J. Wu,[1,64] Lianjie Wu,[19] X. Wu,[12,g] X. H. Wu,[34] Y. H. Wu,[55] Y. J. Wu,[31] Z. Wu,[1,58] L. Xia,[72,58] X. M. Xian,[39] B. H. Xiang,[1,64] T. Xiang,[46,h] D. Xiao,[38,k,l] G. Y. Xiao,[42] H. Xiao,[73] Y. L. Xiao,[12,g] Z. J. Xiao,[41] C. Xie,[42] X. H. Xie,[46,h] Y. Xie,[50] Y. G. Xie,[1,58] Y. H. Xie,[6] Z. P. Xie,[72,58] T. Y. Xing,[1,64] C. F. Xu,[1,64] C. J. Xu,[59] G. F. Xu,[1] M. Xu,[72,58] Q. J. Xu,[16] Q. N. Xu,[30] W. L. Xu,[67] X. P. Xu,[55] Y. Xu,[40] Y. C. Xu,[78] Z. S. Xu,[64] F. Yan,[12,g] L. Yan,[12,g] W. B. Yan,[72,58] W. C. Yan,[81] W. P. Yan,[19] X. Q. Yan,[1,64] H. J. Yang,[51,f] H. L. Yang,[34] H. X. Yang,[1] J. H. Yang,[42] R. J. Yang,[19] T. Yang,[1] Y. Yang,[12,g] Y. F. Yang,[43] Y. X. Yang,[1,64] Y. Z. Yang,[19] Z. W. Yang,[38,k,l] Z. P. Yao,[50] M. Ye,[1,58] M. H. Ye,[8] Junhao Yin,[43] Z. Y. You,[59] B. X. Yu,[1,58,64] C. X. Yu,[43] G. Yu,[13] J. S. Yu,[25,i] M. C. Yu,[40] T. Yu,[73] X. D. Yu,[46,h] C. Z. Yuan,[1,64] J. Yuan,[34] J. Yuan,[45] L. Yuan,[2] S. C. Yuan,[1,64] Y. Yuan,[1,64] Z. Y. Yuan,[59] C. X. Yue,[39] Ying Yue,[19] A. A. Zafar,[74] F. R. Zeng,[50] S. H. Zeng,[63] X. Zeng,[12,g] Y. Zeng,[25,i] Y. J. Zeng,[59] Y. J. Zeng,[1,64] X. Y. Zhai,[34] Y. C. Zhai,[50] Y. H. Zhan,[59] A. Q. Zhang,[1,64] B. L. Zhang,[1,64] B. X. Zhang,[1] D. H. Zhang,[43] G. Y. Zhang,[19] H. Zhang,[81] H. Zhang,[72,58] H. C. Zhang,[1,58,64] H. H. Zhang,[59] H. Q. Zhang,[1,58,64] H. R. Zhang,[72,58] H. Y. Zhang,[1,58] J. Zhang,[59] J. Zhang,[81] J. J. Zhang,[52] J. L. Zhang,[20] J. Q. Zhang,[41] J. S. Zhang,[12,g] J. W. Zhang,[1,58,64] J. X. Zhang,[38,k,l] J. Y. Zhang,[1] J. Z. Zhang,[1,64] Jianyu Zhang,[64] L. M. Zhang,[61] Lei Zhang,[42] P. Zhang,[1,64] Q. Zhang,[19] Q. Y. Zhang,[34] R. Y. Zhang,[38,k,l] S. H. Zhang,[1,64] Shulei Zhang,[25,i] X. M. Zhang,[1] X. Y. Zhang,[40] X. Y. Zhang,[50] Y. Zhang,[73] Y. Zhang,[1] Y. T. Zhang,[81] Y. H. Zhang,[1,58] Y. M. Zhang,[39] Yan Zhang,[72,58] Z. D. Zhang,[1] Z. H. Zhang,[1] Z. L. Zhang,[34] Z. X. Zhang,[19] Z. Y. Zhang,[43] Z. Y. Zhang,[77] Z. Z. Zhang,[45] Zh. Zh. Zhang,[19] G. Zhao,[1] J. Y. Zhao,[1,64] J. Z. Zhao,[1,58] L. Zhao,[1] Lei Zhao,[72,58] M. G. Zhao,[43] N. Zhao,[79] R. P. Zhao,[64] S. J. Zhao,[81] Y. B. Zhao,[1,58] Y. X. Zhao,[31,64] Z. G. Zhao,[72,58] A. Zhemchugov,[36,b] B. Zheng,[73] B. M. Zheng,[34] J. P. Zheng,[1,58] W. J. Zheng,[1,64] X. R. Zheng,[19] Y. H. Zheng,[64] B. Zhong,[41] X. Zhong,[59] H. Zhou,[35,50,o] J. Y. Zhou,[34] S. Zhou,[6] X. Zhou,[77] X. K. Zhou,[6] X. R. Zhou,[72,58] X. Y. Zhou,[39] Y. Z. Zhou,[12,g] Z. C. Zhou,[20] A. N. Zhu,[64] J. Zhu,[43] K. Zhu,[1] K. J. Zhu,[1,58,64] K. S. Zhu,[12,g] L. Zhu,[34] L. X. Zhu,[64] S. H. Zhu,[71] T. J. Zhu,[12,g] W. D. Zhu,[41] W. Z. Zhu,[19] Y. C. Zhu,[72,58] Z. A. Zhu,[1,64] J. H. Zou,[1] and J. Zu[72,58]

(BESIII Collaboration)

[1]*Institute of High Energy Physics, Beijing 100049, People's Republic of China*
[2]*Beihang University, Beijing 100191, People's Republic of China*
[3]*Bochum Ruhr-University, D-44780 Bochum, Germany*
[4]*Budker Institute of Nuclear Physics SB RAS (BINP), Novosibirsk 630090, Russia*
[5]*Carnegie Mellon University, Pittsburgh, Pennsylvania 15213, USA*
[6]*Central China Normal University, Wuhan 430079, People's Republic of China*
[7]*Central South University, Changsha 410083, People's Republic of China*
[8]*China Center of Advanced Science and Technology, Beijing 100190, People's Republic of China*
[9]*China University of Geosciences, Wuhan 430074, People's Republic of China*
[10]*Chung-Ang University, Seoul, 06974, Republic of Korea*
[11]*COMSATS University Islamabad, Lahore Campus, Defence Road, Off Raiwind Road, 54000 Lahore, Pakistan*
[12]*Fudan University, Shanghai 200433, People's Republic of China*
[13]*GSI Helmholtzcentre for Heavy Ion Research GmbH, D-64291 Darmstadt, Germany*
[14]*Guangxi Normal University, Guilin 541004, People's Republic of China*
[15]*Guangxi University, Nanning 530004, People's Republic of China*
[16]*Hangzhou Normal University, Hangzhou 310036, People's Republic of China*
[17]*Hebei University, Baoding 071002, People's Republic of China*
[18]*Helmholtz Institute Mainz, Staudinger Weg 18, D-55099 Mainz, Germany*
[19]*Henan Normal University, Xinxiang 453007, People's Republic of China*
[20]*Henan University, Kaifeng 475004, People's Republic of China*
[21]*Henan University of Science and Technology, Luoyang 471003, People's Republic of China*
[22]*Henan University of Technology, Zhengzhou 450001, People's Republic of China*
[23]*Huangshan College, Huangshan 245000, People's Republic of China*
[24]*Hunan Normal University, Changsha 410081, People's Republic of China*

[25]*Hunan University, Changsha 410082, People's Republic of China*
[26]*Indian Institute of Technology Madras, Chennai 600036, India*
[27]*Indiana University, Bloomington, Indiana 47405, USA*
[28a]*INFN Laboratori Nazionali di Frascati, I-00044, Frascati, Italy*
[28b]*INFN Sezione di Perugia, I-06100, Perugia, Italy*
[28c]*University of Perugia, I-06100, Perugia, Italy*
[29a]*INFN Sezione di Ferrara, I-44122, Ferrara, Italy*
[29b]*University of Ferrara, I-44122, Ferrara, Italy*
[30]*Inner Mongolia University, Hohhot 010021, People's Republic of China*
[31]*Institute of Modern Physics, Lanzhou 730000, People's Republic of China*
[32]*Institute of Physics and Technology, Peace Avenue 54B, Ulaanbaatar 13330, Mongolia*
[33]*Instituto de Alta Investigación, Universidad de Tarapacá, Casilla 7D, Arica 1000000, Chile*
[34]*Jilin University, Changchun 130012, People's Republic of China*
[35]*Johannes Gutenberg University of Mainz, Johann-Joachim-Becher-Weg 45, D-55099 Mainz, Germany*
[36]*Joint Institute for Nuclear Research, 141980 Dubna, Moscow region, Russia*
[37]*Justus-Liebig-Universitaet Giessen, II. Physikalisches Institut, Heinrich-Buff-Ring 16, D-35392 Giessen, Germany*
[38]*Lanzhou University, Lanzhou 730000, People's Republic of China*
[39]*Liaoning Normal University, Dalian 116029, People's Republic of China*
[40]*Liaoning University, Shenyang 110036, People's Republic of China*
[41]*Nanjing Normal University, Nanjing 210023, People's Republic of China*
[42]*Nanjing University, Nanjing 210093, People's Republic of China*
[43]*Nankai University, Tianjin 300071, People's Republic of China*
[44]*National Centre for Nuclear Research, Warsaw 02-093, Poland*
[45]*North China Electric Power University, Beijing 102206, People's Republic of China*
[46]*Peking University, Beijing 100871, People's Republic of China*
[47]*Qufu Normal University, Qufu 273165, People's Republic of China*
[48]*Renmin University of China, Beijing 100872, People's Republic of China*
[49]*Shandong Normal University, Jinan 250014, People's Republic of China*
[50]*Shandong University, Jinan 250100, People's Republic of China*
[51]*Shanghai Jiao Tong University, Shanghai 200240, People's Republic of China*
[52]*Shanxi Normal University, Linfen 041004, People's Republic of China*
[53]*Shanxi University, Taiyuan 030006, People's Republic of China*
[54]*Sichuan University, Chengdu 610064, People's Republic of China*
[55]*Soochow University, Suzhou 215006, People's Republic of China*
[56]*South China Normal University, Guangzhou 510006, People's Republic of China*
[57]*Southeast University, Nanjing 211100, People's Republic of China*
[58]*State Key Laboratory of Particle Detection and Electronics, Beijing 100049, Hefei 230026, People's Republic of China*
[59]*Sun Yat-Sen University, Guangzhou 510275, People's Republic of China*
[60]*Suranaree University of Technology, University Avenue 111, Nakhon Ratchasima 30000, Thailand*
[61]*Tsinghua University, Beijing 100084, People's Republic of China*
[62a]*Turkish Accelerator Center Particle Factory Group, Istinye University, 34010, Istanbul, Turkey*
[62b]*Near East University, Nicosia, North Cyprus, 99138, Mersin 10, Turkey*
[63]*University of Bristol, H H Wills Physics Laboratory, Tyndall Avenue, Bristol, BS8 1TL, United Kingdom*
[64]*University of Chinese Academy of Sciences, Beijing 100049, People's Republic of China*
[65]*University of Groningen, NL-9747 AA Groningen, The Netherlands*
[66]*University of Hawaii, Honolulu, Hawaii 96822, USA*
[67]*University of Jinan, Jinan 250022, People's Republic of China*
[68]*University of Manchester, Oxford Road, Manchester, M13 9PL, United Kingdom*
[69]*University of Muenster, Wilhelm-Klemm-Strasse 9, 48149 Muenster, Germany*
[70]*University of Oxford, Keble Road, Oxford OX13RH, United Kingdom*
[71]*University of Science and Technology Liaoning, Anshan 114051, People's Republic of China*
[72]*University of Science and Technology of China, Hefei 230026, People's Republic of China*
[73]*University of South China, Hengyang 421001, People's Republic of China*
[74]*University of the Punjab, Lahore-54590, Pakistan*
[75a]*University of Turin and INFN, University of Turin, I-10125, Turin, Italy*
[75b]*University of Eastern Piedmont, I-15121, Alessandria, Italy*
[75c]*INFN, I-10125, Turin, Italy*
[76]*Uppsala University, Box 516, SE-75120 Uppsala, Sweden*

[77]*Wuhan University, Wuhan 430072, People's Republic of China*
[78]*Yantai University, Yantai 264005, People's Republic of China*
[79]*Yunnan University, Kunming 650500, People's Republic of China*
[80]*Zhejiang University, Hangzhou 310027, People's Republic of China*
[81]*Zhengzhou University, Zhengzhou 450001, People's Republic of China*

[a]Deceased.
[b]Also at the Moscow Institute of Physics and Technology, Moscow 141700, Russia.
[c]Also at the Novosibirsk State University, Novosibirsk, 630090, Russia.
[d]Also at the NRC "Kurchatov Institute," PNPI, 188300, Gatchina, Russia.
[e]Also at Goethe University Frankfurt, 60323 Frankfurt am Main, Germany.
[f]Also at Key Laboratory for Particle Physics, Astrophysics and Cosmology, Ministry of Education; Shanghai Key Laboratory for Particle Physics and Cosmology; Institute of Nuclear and Particle Physics, Shanghai 200240, People's Republic of China.
[g]Also at Key Laboratory of Nuclear Physics and Ion-beam Application (MOE) and Institute of Modern Physics, Fudan University, Shanghai 200443, People's Republic of China.
[h]Also at State Key Laboratory of Nuclear Physics and Technology, Peking University, Beijing 100871, People's Republic of China.
[i]Also at School of Physics and Electronics, Hunan University, Changsha 410082, China.
[j]Also at Guangdong Provincial Key Laboratory of Nuclear Science, Institute of Quantum Matter, South China Normal University, Guangzhou 510006, China.
[k]Also at MOE Frontiers Science Center for Rare Isotopes, Lanzhou University, Lanzhou 730000, People's Republic of China.
[l]Also at Lanzhou Center for Theoretical Physics, Lanzhou University, Lanzhou 730000, People's Republic of China.
[m]Also at the Department of Mathematical Sciences, IBA, Karachi 75270, Pakistan.
[n]Also at Ecole Polytechnique Federale de Lausanne (EPFL), CH-1015 Lausanne, Switzerland.
[o]Also at Helmholtz Institute Mainz, Staudinger Weg 18, D-55099 Mainz, Germany.